

Supporting Information S2 - Lotka-Volterra food web dynamics with moderately complex structure

Supporting Information for *How do MAR(1) models cope with hidden nonlinearities in ecological dynamics?*
Grégoire Certain, Frédéric Barraquand and Anna Gårdmark, *Methods in Ecology and Evolution* 2018.

The associated code has DOI:10.5281/zenodo.1218024, available at <https://zenodo.org/record/1218024>.
The corresponding GitHub repository can be browsed at https://github.com/fbarraquand/MAR_foodWeb_MEE.

1 Introduction - food web model construction

The food web dynamics has been modelled in the following manner

- A real network topology (Fig. 1) has been considered, based on the food web of Gatun lake (Aufderheide *et al.*, 2013). It has 12 species and a connectance of 21% (27% with self-regulation terms)¹. 4 species (1/3) are affected by the environmental variable.
- Based on this food web topology, parameters have been drawn at random within bounds for each simulation, for both the interaction matrix and the environmental effects.
- We used parameters maintaining feasibility of the equilibrium, i.e. strictly positive abundances for all species - as in the main text. Parameter bounds were chosen so that all simulations produce realistic time series (i.e., top predators fluctuate mildly, while r-strategists lower down the food chain can have more variable dynamics).

2 The general Lotka-Volterra-Ricker (LVR) food web model and its log-linearized Jacobian matrix

We used a general LVR model (with environmental effects) to simulate the food web, as it allows for non-linear dynamics but maintains analytical tractability, as well as a connection to the results of the main text. The LVR model is written in logarithmic scale as:

$$\mathbf{n}_{t+1} = \mathbf{n}_t + \mathbf{r} + \mathbf{C}\mathbf{u}_t + \mathbf{A}\mathbf{N}_t + \mathbf{w}_t, \mathbf{w}_t \sim \text{MVN}(0, \Sigma) \quad (1)$$

where the vector of untransformed abundances is $\mathbf{N}_t = (N_{1t}, \dots, N_{St})^T = (e^{n_{1t}}, \dots, e^{n_{St}})^T$. The matrix $\mathbf{A} = (\alpha_{ij})$ contains all the species interaction coefficients. We assume that the kill rate of an individual predator of species j on prey from species i is $\beta_{ij}N_i$. Because the dynamics are of the Lotka-Volterra predation type, we have

$$\alpha_{ij} = -\beta_{ij} \text{ if prey } i \text{ is eaten by } j \quad (2)$$

$$+\varepsilon_{ij}\beta_{ji} \text{ if predator } i \text{ eats prey } j \quad (3)$$

A term $-\beta_{ij}$ may likewise model competitive per capita effects of species j on species i . We assume that $\beta_{ij} = 0$ unless $i = j$. An intraspecific competition coefficient $\beta_{ii} > 0$ term combined with $r_i > 0$ ensures logistic growth in absence of the other species, which allows to create feasible food webs (i.e., $N_i^* > 0$ for all i). This was especially important for the base of the food web (see ‘Parameters’ below). Regarding the efficiency ε_{ij} of predator i on

¹Other choices, such as modular networks with clusters of strong interactors linked by weaker inter-cluster ties, are possible. However, they would be essentially similar to considering several interacting small modules of 2 or 3 species. The chosen food web involves some degree of omnivory and resource competition at intermediate trophic levels, which we view as relatively common in real food webs.

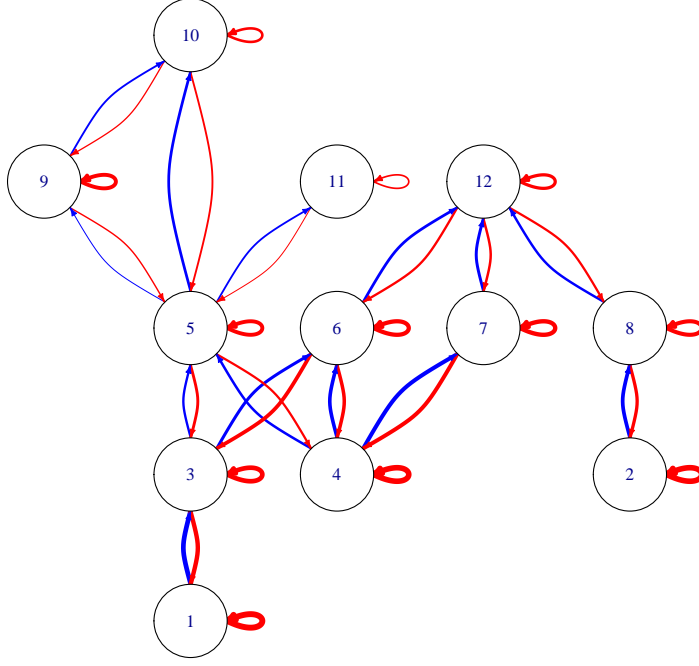


Figure 1: Food web topology and interaction strength pattern (red: negative feedback, blue: positive feedback; width of arrows proportional to $\log(\text{interaction strength})$ as indicated by \mathbf{J} , for one randomly created parameter set)

prey j , there are different options. Setting $\varepsilon_{ij} = \varepsilon_i$ assumes that the predator i transforms all prey j with equal efficiency, with predators varying in their energetic conversion coefficient. $\varepsilon_{ij} = \varepsilon_j$ assumes on the contrary that prey have varying energetic content, but predators have identical conversion efficiencies. Given the many choices possible, we preferred to set $\varepsilon_{ij} = \varepsilon = 0.1$ for simplicity.

Deriving the Jacobian matrix on a log-scale

Our model belongs to the general family of coupled nonlinear stochastic difference equations

$$n_{i,t+1} = f_i((n_{k,t})_{k \in [1,S]}) + \epsilon_{i,t} \quad (4)$$

where $\epsilon_{i,t}$ is an additive, centered Gaussian noise term. For this and similar models, the Jacobian element is therefore $J_{ij} = \frac{\partial f_i}{\partial n_j} |_{\mathbf{n}=\mathbf{n}^*}$. In the LVR model, we have $f_i(\mathbf{n}) = n_i + \mathbf{c}_{i\bullet} \mathbf{u}_t + \alpha_{i\bullet} \mathbf{N}_t$ with $\alpha_{i\bullet} \mathbf{N}_t = \sum_{k=1}^S \alpha_{ik} N_{k,t}$. This implies that

$$\frac{\partial f_i}{\partial n_j} = \underbrace{\frac{\partial n_i}{\partial n_j}}_{=0 \text{ if } i \neq j} + \underbrace{\frac{\partial (r_i + \mathbf{c}_{i\bullet} \mathbf{u}_t)}{\partial n_j}}_{=0} + \sum_{k=1}^S \alpha_{ik} \frac{\partial e^{n_k}}{\partial n_j} = \delta_{ij} + \alpha_{ij} e^{n_j} \quad (5)$$

with $\delta_{ij} = 1$ if $i = j$, and $\delta_{ij} = 0$ otherwise. Hence,

$$J_{ij} = \delta_{ij} + \alpha_{ij} e^{n_j^*} \quad (6)$$

Computation of the equilibrium point

We have at equilibrium

$$\mathbf{0} = \mathbf{r} + \mathbf{C}\mathbf{u}^* + \mathbf{A}\mathbf{N}^* = \mathbf{r} + \mathbf{A}\mathbf{N}^* \quad (7)$$

so that

$$\mathbf{N}^* = \mathbf{A}^{-1}(-\mathbf{r}) \quad (8)$$

We check notably the feasibility (strictly positive abundances for all species) of the equilibrium.

Interaction matrix A

Assuming there are only trophic relationships (no direct competition between species) and within-species regulation, the interaction matrix now writes

$$A = \begin{pmatrix} -\beta_{11} & 0 & -\beta_{31} & 0 & 0 & 0 & 0 & 0 & 0 & 0 & 0 & 0 & 0 \\ 0 & -\beta_{22} & 0 & 0 & 0 & 0 & 0 & -\beta_{28} & 0 & 0 & 0 & 0 & 0 \\ \varepsilon_{31}\beta_{13} & 0 & -\beta_{33} & 0 & -\beta_{35} & -\beta_{36} & 0 & 0 & 0 & 0 & 0 & 0 & 0 \\ 0 & 0 & 0 & -\beta_{44} & -\beta_{45} & -\beta_{46} & -\beta_{47} & 0 & 0 & 0 & 0 & 0 & 0 \\ 0 & 0 & \varepsilon_{53}\beta_{35} & \varepsilon_{54}\beta_{45} & -\beta_{55} & 0 & 0 & 0 & -\beta_{59} & -\beta_{5,10} & -\beta_{5,11} & 0 & 0 \\ 0 & 0 & \varepsilon_{63}\beta_{36} & \varepsilon_{64}\beta_{46} & 0 & -\beta_{66} & 0 & 0 & 0 & 0 & 0 & 0 & -\beta_{6,12} \\ 0 & 0 & 0 & \varepsilon_{74}\beta_{47} & 0 & 0 & -\beta_{77} & 0 & 0 & 0 & 0 & 0 & -\beta_{7,12} \\ 0 & \varepsilon_{82}\beta_{28} & 0 & 0 & 0 & 0 & 0 & -\beta_{88} & 0 & 0 & 0 & 0 & -\beta_{8,12} \\ 0 & 0 & 0 & 0 & \varepsilon_{95}\beta_{59} & 0 & 0 & 0 & -\beta_{99} & -\beta_{9,10} & 0 & 0 & 0 \\ 0 & 0 & 0 & 0 & \varepsilon_{10,5}\beta_{5,10} & 0 & 0 & 0 & \varepsilon_{10,9}\beta_{9,10} & -\beta_{10,10} & 0 & 0 & 0 \\ 0 & 0 & 0 & 0 & \varepsilon_{11,5}\beta_{5,11} & 0 & 0 & 0 & 0 & 0 & 0 & -\beta_{11,11} & 0 \\ 0 & 0 & 0 & 0 & 0 & \varepsilon_{12,6}\beta_{6,12} & \varepsilon_{12,7}\beta_{7,12} & \varepsilon_{12,8}\beta_{8,12} & 0 & 0 & 0 & 0 & -\beta_{12,12} \end{pmatrix} \quad (9)$$

Environmental effects

Species 1, 2, 4 and 11 were chosen to be forced (simultaneously) by the environmental variable. The idea was to force three species at the base of the food web (to maintain a connection to the results of our main text) and also a species at the top of the food web.

Parameters

We chose parameter values partially at random. The mean values of intraspecific interaction strength, β_{intra} , was set to 0.3 for all species but species 10,11 and 12 that had $\beta_{\text{intra}} = 0.9$. Strong regulation is indeed needed at the top of the food web for stability. The mean interspecific interaction strength was set to 0.1. Then each interaction coefficient was drawn as $\beta_{ij} = \delta_{ij}\beta_{\text{intra}} + (1 - \delta_{ij})\beta_{\text{inter}} + \text{Unif}(-0.1, 0.1)$, which is then converted into α_{ij} according to eq. 2.

The intrinsic growth rates were different for the different trophic levels

- r_{prey} was 2 for species 1 and 1 for species 2 and 4.
- $r_{\text{intermediate}} \sim \text{Unif}(0.01, 0.05)$. Intermediate species are assumed to reproduce very little if their prey are not present in the food web. We did not include negative r_i (death only in absence of prey) because these had a detrimental effect on the feasibility of the food web. Also, a food web is never a complete representation of reality, thus a negative r_i does not necessarily makes sense if one thinks predator i might access at times prey outside of the web (e.g., Erbach *et al.*, 2013).
- $r_{\text{top}} = 0.001$ to 0.0001. The intrinsic growth rate of the top predators is considered to be very low, in line with the fact that they need the lower trophic levels to reproduce, and their life histories are usually much slower.

Length of the time series The number of timesteps was first set to 100, as in the two-species experiment. This resulted in poor, highly variable estimates including in the Gompertz model ² (fraction of correctly detected signs closer to 0.5 than 1 for most interactions). A time series length of 800 was therefore chosen to provide an amount of data, in relation to the number of parameters estimated, that was comparable to the 2-species models of the main text. In the following, we report the results for $t_{\text{max}} = 800$. As there are intrinsically more constraints for the

²Constructing high-dimensional models for short time series typically require some procedure to “shrink” the estimates, i.e., correct for the added variance in estimates at low sample sizes. Classical choices of regularization techniques (e.g., Basu *et al.*, 2015) include ridge regression, the LASSO (which performs model selection at the same time), as well as some other techniques with a Bayesian perspective (e.g., Mutshinda *et al.*, 2011; Ovaskainen *et al.*, 2017)

feasibility of the equilibrium point (and the perturbed state after the PRESS) for a 12-species than 2 or 3 species food web, less variation in parameter values was considered than in the 2-species simulations³.

CONTROL GOMPERTZ SIMULATION

In order to see what properties of the estimates can be attributed specifically to the LVR model, we also produced a Gompertz food web dynamics. Due to the difficulties in specifying a Gompertz food web (see Discussion in main text), we use for \mathbf{B} the Jacobian of the LVR model (eq. 6) with the abovementioned parameters.

3 Model fitting

We used, as in the main text, MARSS for model fitting (Holmes *et al.*, 2014). We chose two contrasted MAR(1) model formulations, one in which the topology of the net interaction matrix was fully unknown, with a full \mathbf{B} and a full \mathbf{C} matrix that could take any values, and one in which it was fully known, with sparse \mathbf{B} and \mathbf{C} matrices, constrained by the known topology of the food web (i.e., b_{ij} was set to zero if α_{ij} was set to zero; a similar rule was used for the environmental effect matrix \mathbf{C}). Contrasting these two cases reveals how hidden non-linearities challenge the estimation of MAR models under contrasted scenarios of prior knowledge on ecological interactions.

We are aware that fitting large MAR models without long time series - and even with relatively long ones of several hundred time steps - can generate massive overparameterization (Michailidis & d'Alché Buc, 2013). For instance, fitting a full 12-species MAR models to a 100 timepoints time series requires estimating more parameters than time steps and require regularization techniques (e.g., Basu *et al.*, 2015). With the 800 timesteps chosen, such problems remain moderate.

We fitted MAR(1) models to 100 LVR and 100 Gompertz simulations, each with randomly chosen parameters sets (as in the main text). Each time, both the MAR(1) models with the known and unknown topology were fitted, for $t_{\max} = 800$. This resulted therefore in $2 \times 2 \times 100 = 400$ MAR(1) model fits (considering only the case with 800 timesteps for which we present the results below). See the GitHub/Zenodo repository for the details of the simulation, model fitting and model comparison⁴. In the following, we focus on the main results of our food web simulation and model fitting experiment.

4 Results of the food web model fitting, PRESS prediction and discussion

There are two complementary ways in which the estimation results (e.g., \mathbf{B} matrix coefficients) can be presented:

1. Within-repeats summary statistics, such as the correlation between \mathbf{B} and \mathbf{J} of diagonal and off-diagonal elements, for one given simulation run (i.e., one repeat).
2. Across-repeats summary statistics. These include the correlation between $b_{i,j}$ and $j_{i,j}$ across repeats, as we do in the main text, the fraction of well-recovered signs, the fraction of \mathbf{J} elements out of 95% CIs for \mathbf{B} .

Both within- and across-repeats statistics contain relevant information: within-repeats statistics allow to identify simulation runs where the estimation of most elements is good or poor, while across-repeats allow to identify matrix elements that were systematically well- or poorly-estimated across simulation runs.

We note, however, that presenting correlations calculated using the whole \mathbf{B} matrix for one simulation run, as done recently by Ovaskainen *et al.* (2017), unfortunately tends to present an over-optimistic picture of the estimation of interspecific interactions. The correlation $\text{Cor}(\text{vec}(\mathbf{B}), \text{vec}(\mathbf{J}))$, for one repeat, is indeed often driven by a set of points near (0,0) and a set of points near (1,1) (Fig. 2 and Table 1). We therefore recommend to at least separate diagonal from off-diagonal elements when presenting correlations (as we do below in Table 1).

INTERACTION PARAMETERS - B MATRIX

Overall, we recover the results of the main text for 2-species models:

³It may be possible to construct strongly interacting webs by allowing species extinction and a real assembly process, starting from a larger species pool. This would, however, create webs with different structure for each parameter set and impede element-by-element comparison, as we do here and in the main text.

⁴https://github.com/fbarraquand/MAR_foodWeb_MEE, version of record <https://zenodo.org/record/1218024>

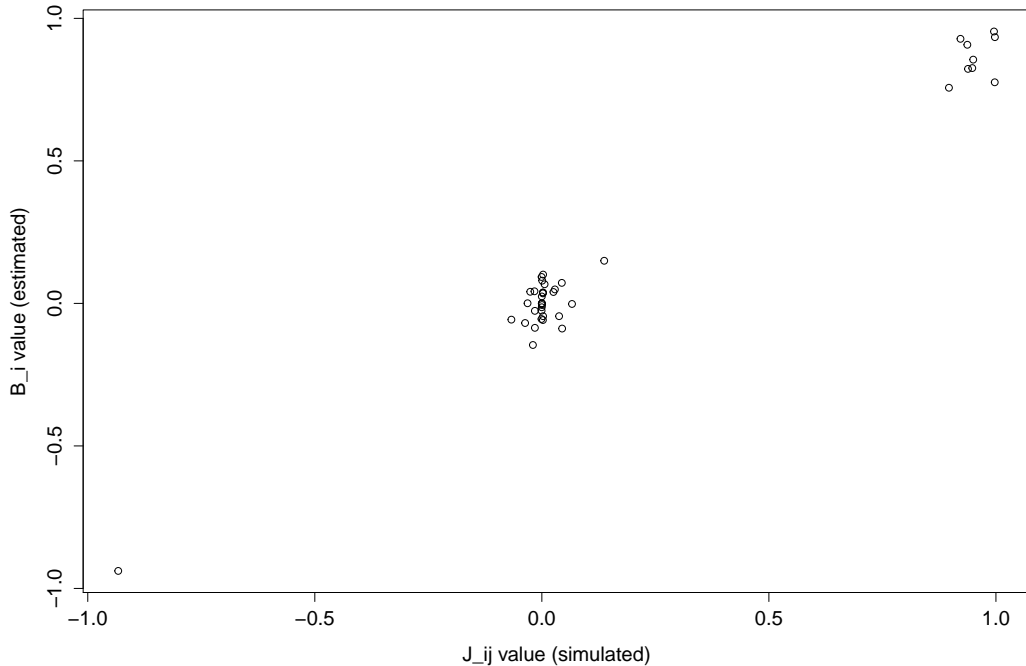


Figure 2: Estimated vs. simulated values of \mathbf{B} for a Gompertz simulation. The overall correlation (as reported in Ovaskainen *et al.*, 2017) is 98% (94% for an unknown network topology), even though the correlation between interspecific elements (center cluster) is merely 50% (29% for unknown topology).

- There is a slight underestimation of interspecific interaction strengths in the LVR model (Fig. 3), as for the two-species LVR model MAR estimates. This is less visible than in the two-species model, because some interaction strengths are very small and the range of variation in interaction strength is overall smaller than in the two-species example. The underestimation is noticeable for, e.g., interactions between species 1 and 3 (Fig. 3).
- The percentage of correctly identified signs across simulations is lower than in our 2-species system but still acceptable for the lower part of the food web (78% averaged across non-zero \mathbf{J} elements overall). Sign recovery varies quite a bit in relation to interaction strength: most reasonably strong interactions, above 10^{-1} in absolute value, are well recovered in sign, Fig. 4. Effects of prey on predator are weaker than those of predator on prey, and tend to be less well recovered, especially at the top of the food web. This is true even in the theoretical formulation of net interaction strength. We have indeed $J_{ij} = \epsilon\beta_{ji}\exp(n_j^*)$ with $\epsilon = 0.1$ and very low n_j^* for predators. The conclusion is therefore that effects prey \rightarrow predator tend to be less well recovered because they are intrinsically weaker, at least when constraining our food web model to produce lifelike species abundance distributions, with an Eltonian biomass pyramid forbidding large predator abundances.
- The results are similar for a Gompertz model whose coefficients are those of the Jacobian of the LVR model. For the Gompertz case, there is less bias (underestimation) in the estimation of the \mathbf{B} elements (which is logical) but more variance in the estimates (Fig. 5).
- The correlation between \mathbf{B} and \mathbf{J} off-diagonal elements for a given simulation and parameter set varies quite widely (from 90% to negative values, Table 1). This strongly suggests that some simulations - even in the Gompertz case - have poorly identified parameter combinations. These ‘bad apples’ potentially contribute heavily to the decrease in overall MAR model performance, but more work is needed to investigate the variance in estimates across parameter sets.
- Overcompensation, at least in the basal species for which the intrinsic growth rate is large ($r = 2$), was well identified. Note that species 2 and 4 have $r = 1$, which is at the boundary of overcompensation; therefore it

is normal that for those species overcompensation is less clear.

- Cases with dominant eigenvalue above 1 in norm result in a mismatch between \mathbf{B} and \mathbf{J} (not shown, requires additional parameter values), as for the LVR-T2-cycle in the main text.
- The ‘full \mathbf{B} matrix’ model seems to identify correctly the interaction sign and strength in the Gompertz case (Fig. 6) even slightly better than the web with known topology. In the LVR case, the fraction of correctly identified signs for each element of interest is similar between a priori known and unknown web topologies (Table 2). Thus far, specifying the network topology has had little impact on the quality of the estimates, for this food web simulation. Of course, there are some false positives (significant interactions at a 95% level) in \mathbf{B} elements without constraints on \mathbf{B} , but they seem to have moderate impact on sign recovery.
- Statistical techniques are available for regularized estimation of MAR(1) models. They would improve estimates of \mathbf{B} without a knowledge of the web topology a priori (e.g., sparse modelling, dimension reduction through clustering; Michailidis & d’Alché Buc, 2013; Basu *et al.*, 2015; Ovaskainen *et al.*, 2017) and their evaluation would need to be extended. For example, there is no evaluation in Ovaskainen *et al.* (2017) of interaction sign inference (sign is arguably key to biological interpretation), only the overall correlation between \mathbf{B} elements. Unfortunately, as we show in Fig. 2, a ‘raw’ correlation between \mathbf{B} and \mathbf{J} elements of a single MAR(1) model is not a reliable tool to evaluate properly the quality of off-diagonal (interspecific) coefficients.

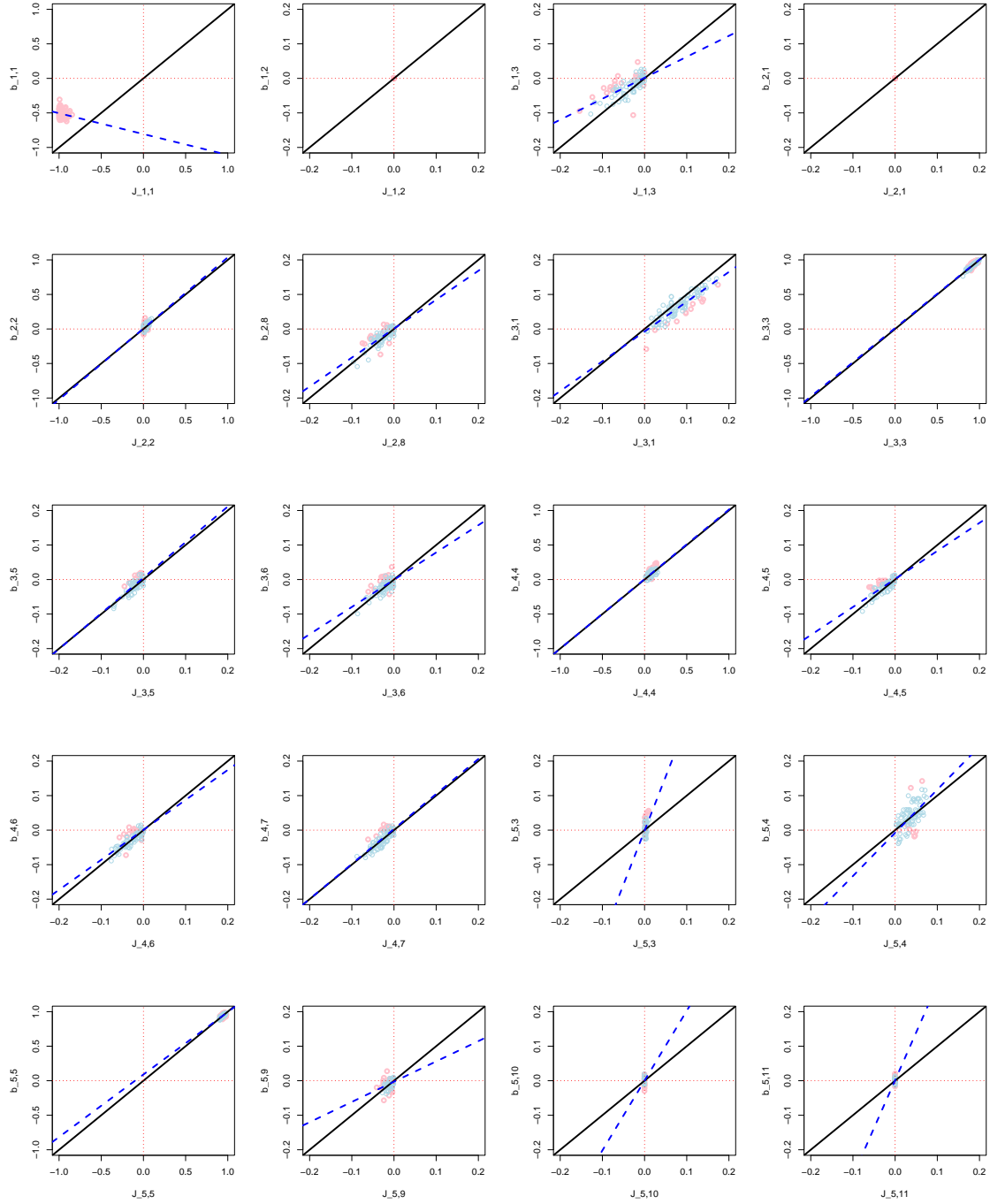


Figure 3: **B vs J, estimation for the LVR model.** Known food web topology, 800 timesteps.. Only the first non-zero J elements are presented. Blue points: J element within B's CIs; pink: not within B's CIs. Blue dotted line: regression $b_{ij} \sim j_{ij}$.

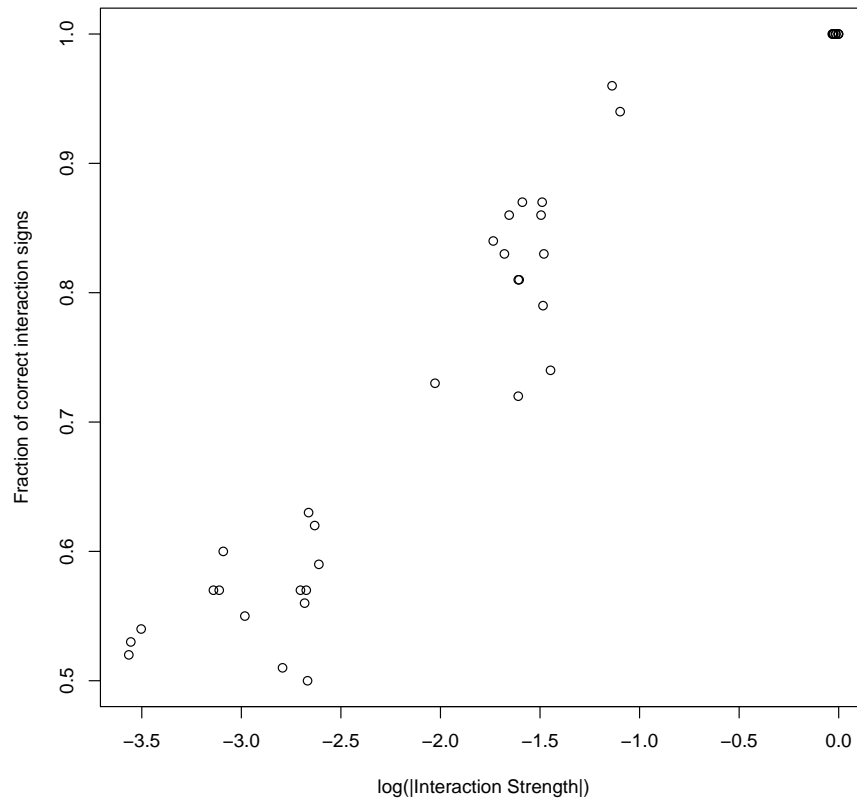


Figure 4: Relationship between the fraction of correctly identified interaction signs and the log(interaction strength).

rep.	raw_correl	signif_correl	diag_correl	upperD_correl	lowerD_correl	offD_correl	offDiag_dist	max_eigB	max_eigJ
1	0.9895	0.9893	0.9878	0.8104	0.8557	0.8281	0.4313	0.9943	0.9994
2	0.9879	0.9875	0.9904	0.9876	0.9723	0.9684	0.2614	0.9966	0.9987
3	0.9929	0.9929	0.9921	0.9596	0.8702	0.8906	0.3367	0.9926	0.9999
4	0.9908	0.9907	0.9924	0.7732	0.874	0.8454	0.2669	0.9931	0.9984
5	0.989	0.9885	0.9895	0.513	0.9095	0.8234	0.435	0.9972	0.9977
6	0.9851	0.9853	0.9866	-0.0625	0.2027	0.183	0.227	0.9997	0.9984
7	0.993	0.9935	0.9966	0.8862	0.8567	0.8611	0.5384	0.996	0.9985
8	0.9828	0.9823	0.9835	0.3935	0.6954	0.5799	0.3611	0.9977	0.9987
9	0.9726	0.972	0.9636	0.7947	0.6782	0.7337	0.2842	0.9942	0.9998
10	0.9909	0.9908	0.9913	0.9255	0.7828	0.8391	0.2868	0.992	0.9991
11	0.9898	0.9896	0.992	0.9151	0.5124	0.6385	0.3503	0.9981	0.9983
12	0.9873	0.9874	0.9849	0.5964	NA	0.3249	0.3884	0.999	0.9988
13	0.9907	0.9904	0.9892	0.5968	0.7971	0.7349	0.3023	0.9949	0.9991
14	0.9801	0.9799	0.9842	0.0011	0.3027	0.2479	0.3892	0.9966	0.9997
15	0.9887	0.9885	0.9902	0.468	0.5562	0.5089	0.3483	0.9929	0.9984
16	0.9855	0.9851	0.989	0.9078	0.5661	0.7447	0.3138	1.0008	0.9979
17	0.9862	0.9861	0.989	0.9175	0.8334	0.8682	0.2962	0.9988	0.9995
18	0.9908	0.9905	0.9911	0.8209	0.5365	0.6448	0.2329	0.9927	0.9994
19	0.984	0.9836	0.9868	0.8878	0.6344	0.7188	0.3625	0.9914	0.9995
20	0.9873	0.9873	0.9953	0.7585	0.7189	0.7222	0.4301	0.9902	1
21	0.983	0.9833	0.9875	0.3765	-0.1329	-0.0496	0.3227	0.9973	0.9998
22	0.9913	0.9913	0.9915	0.5879	0.9358	0.8398	0.3433	0.9954	0.9992
23	0.9841	0.9841	0.9855	0.7648	0.885	0.778	0.3562	0.9955	0.9995
24	0.9898	0.9898	0.9932	0.7816	0.6881	0.6744	0.3649	0.9975	0.999
25	0.9901	0.9902	0.9927	0.977	0.941	0.955	0.3382	0.9926	0.9972

Table 1: Correlation coefficients between \mathbf{B} and \mathbf{J} elements. We present raw correlations as done in Ovaskainen *et al.* (2017), correlations between \mathbf{J} elements (second column) and 95% significant elements of \mathbf{B} (third column), correlation between diagonal elements only (fourth), upper and lower diagonal elements (fifth and sixth), and off-diagonal elements (union of lower and upper triangular matrices, seventh column). Each correlation is computed for each repeat (i.e., each model simulation and MAR(1) model fit), and we also present a measure of distance of distance between \mathbf{B} and \mathbf{J} off diagonal (sum of $\text{abs}(\mathbf{B}-\mathbf{J})$ for non-diagonal elements, eighth column) as well as stability properties (norm of the dominant eigenvalue for \mathbf{B} and \mathbf{J} , ninth and tenth columns). We present the 25 first repeats, out of 100, for illustration. Full tables are available in the code repository.

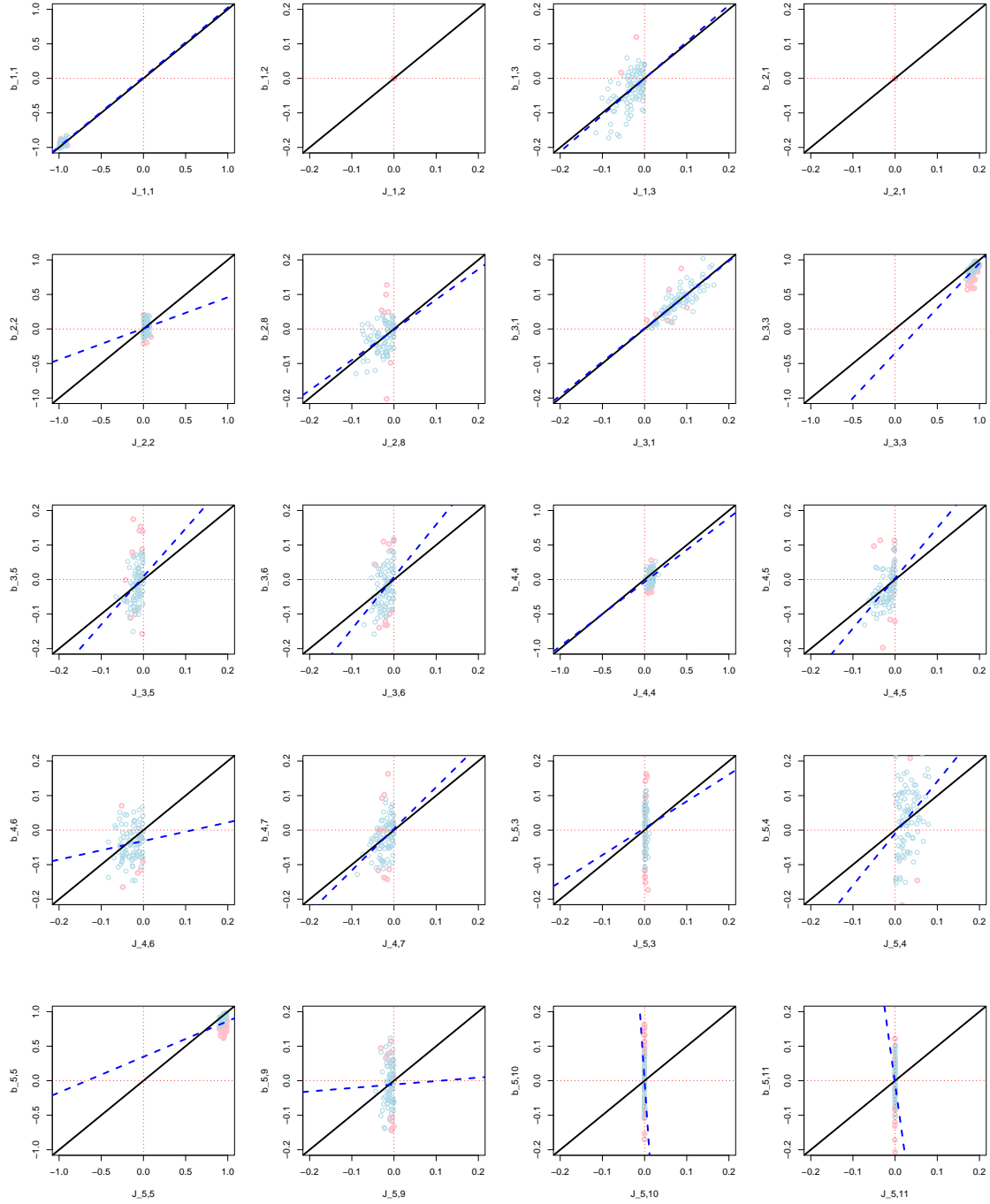


Figure 5: **B vs J, estimation for the Gompertz model.** Known food web topology, 800 timesteps. Only the first non-zero J elements are presented. Blue points: J element within B's CIs; pink: not within B's CIs. Blue dotted line: regression $b_{ij} \sim j_{ij}$.

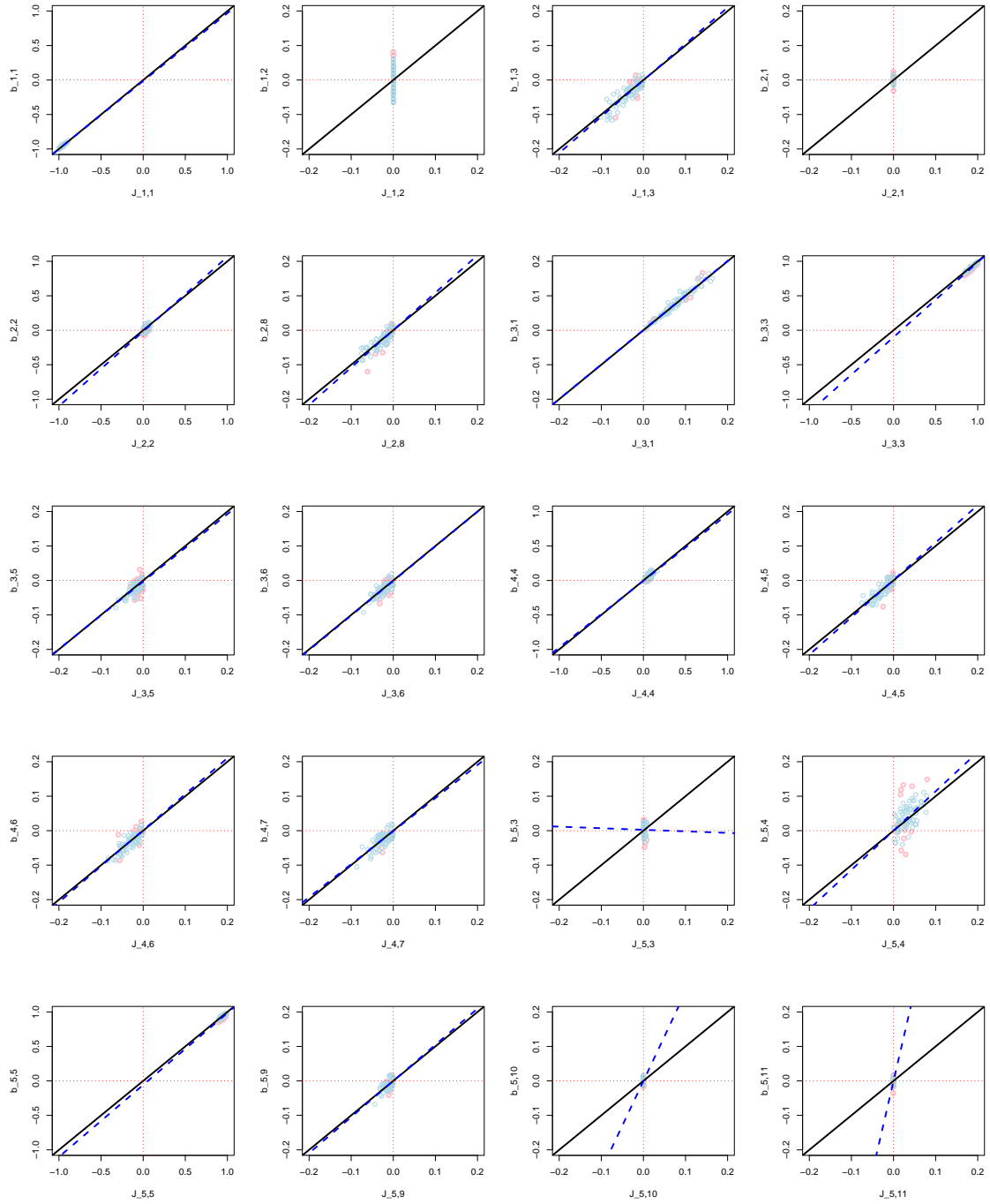


Figure 6: \mathbf{B} vs \mathbf{J} , estimation for the Gompertz model. Unknown food web topology, 800 timesteps.

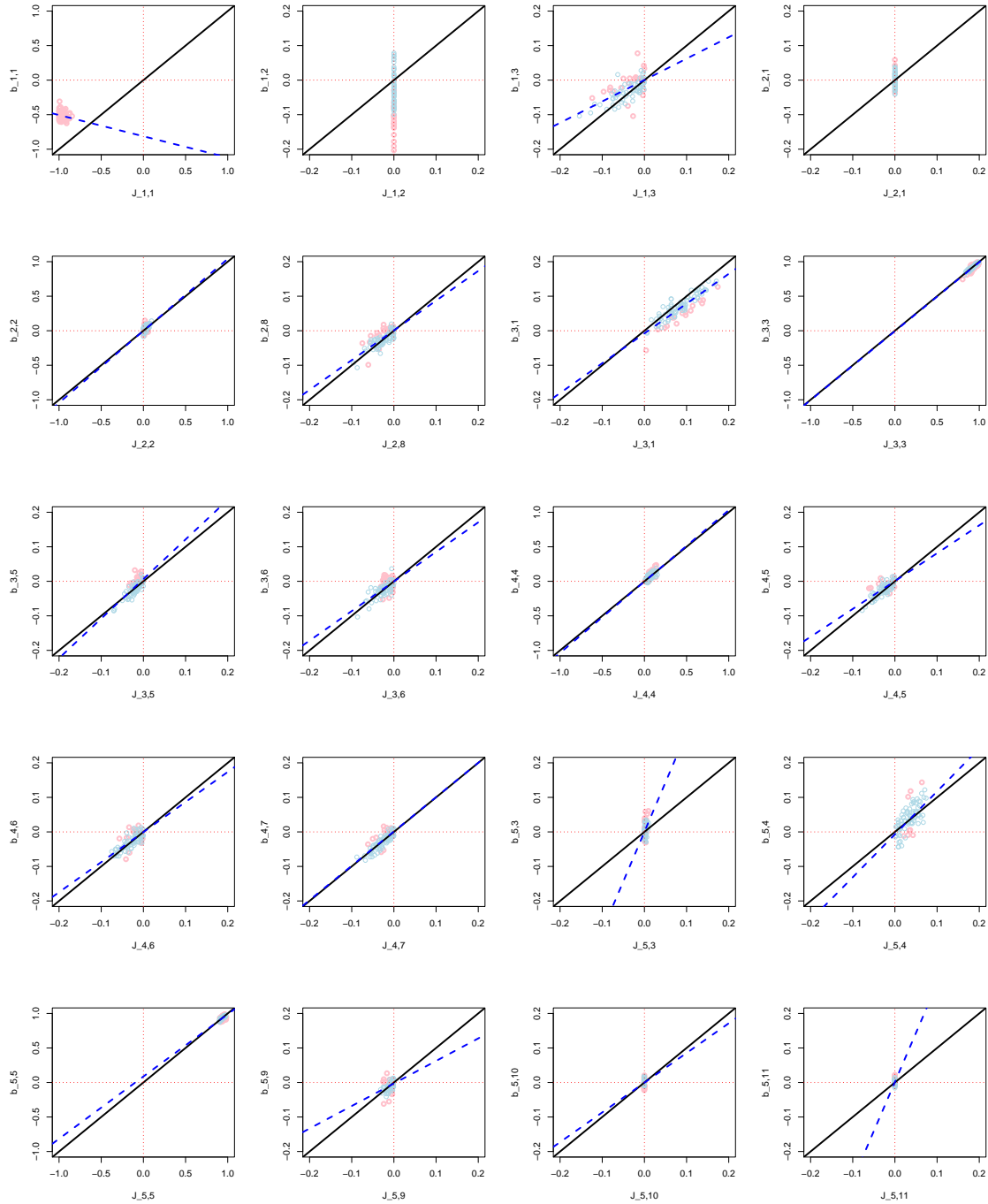


Figure 7: **B** vs **J**, estimation for the LVR model. Unknown food web topology, 800 timesteps.

ENVIRONMENTAL EFFECTS - C MATRIX

The environmental forcing of population growth rates is overall very well recovered - both in sign and magnitude - when the topology is known, for the LVR model (Fig. 8), except for the weak environmental effect on species 11 (which could have been expected).

B element	Known web topology	Unknown topology
b_1,1	1	1
b_1,2	1	NA
b_1,3	0.74	0.7
b_2,1	1	NA
b_2,2	0.72	0.67
b_2,8	0.81	0.77
b_3,1	0.94	0.94
b_3,3	1	1
b_3,5	0.84	0.81
b_3,6	0.83	0.8
b_4,4	0.96	0.93
b_4,5	0.86	0.81
b_4,6	0.87	0.83
b_4,7	0.81	0.83
b_5,3	0.63	0.59
b_5,4	0.79	0.79
b_5,5	1	1
b_5,9	0.73	0.71
b_5,10	0.54	0.5
b_5,11	0.53	0.54
b_6,3	0.57	0.62
b_6,4	0.87	0.88
b_6,6	1	1
b_6,12	0.6	0.6
b_7,4	0.83	0.83
b_7,7	1	1
b_7,12	0.57	0.58
b_8,2	0.86	0.85
b_8,8	1	1
b_8,12	0.57	0.57
b_9,5	0.51	0.54
b_9,9	1	1
b_9,10	0.52	0.48
b_10,5	0.56	0.56
b_10,9	0.55	0.53
b_10,10	1	1
b_11,5	0.57	0.58
b_11,11	1	1
b_12,6	0.59	0.57
b_12,7	0.62	0.63
b_12,8	0.5	0.5
b_12,12	1	1

Table 2: Fraction of correctly identified net interaction signs, across repeats, for the various elements of \mathbf{B} that correspond to *a priori* non-zero interactions

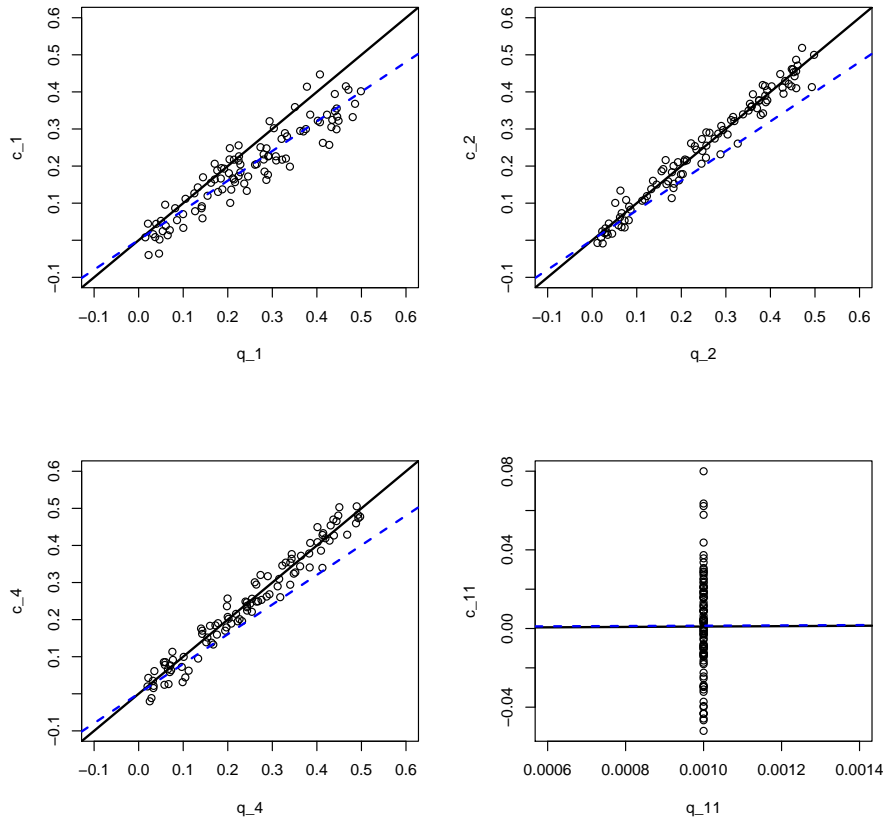


Figure 8: \mathbf{C} vs \mathbf{Q} , estimation for the LVR model. Known environmental effects topology.

For the Gompertz model, this recovery is unbiased and extremely good (Fig. 9). Although the patterns of environmental forcing are arguably simple here, there seem much better recovered - much less ambiguous - than the interactions between species.

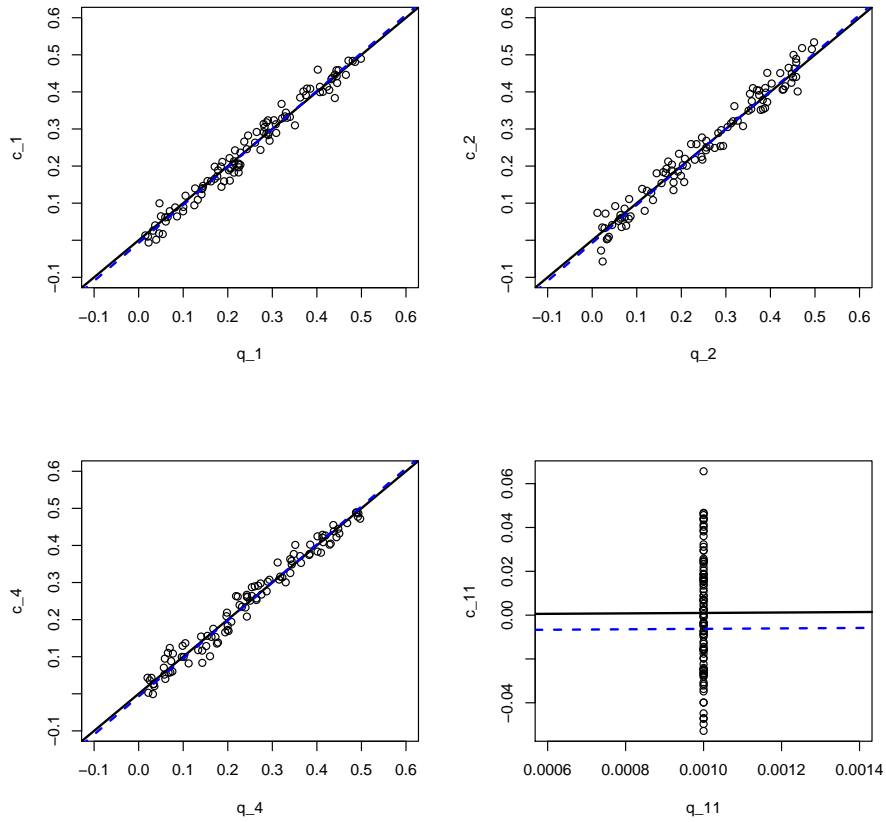


Figure 9: **C vs Q, estimation for the Gompertz model.** Known environmental effects topology.

With an unknown environmental effect topology and still the Gompertz model, we find virtually indistinguishable results from the known topology case. The detailed results for all elements (including species 3,5,6,7,8,9,10,12) reveal a rate of false positives of 30%, as evidenced by values significantly different from zero at the 95% significance threshold. These values may seem high, but they are in fact of no importance. Only 1 coefficient in 800 reaches the absolute value 0.1, thus the false positives represent quantitatively small effects compared to the simulated effects on species 1, 2, and 4 (the latter being correctly identified as both statistically significant and having large effect sizes).

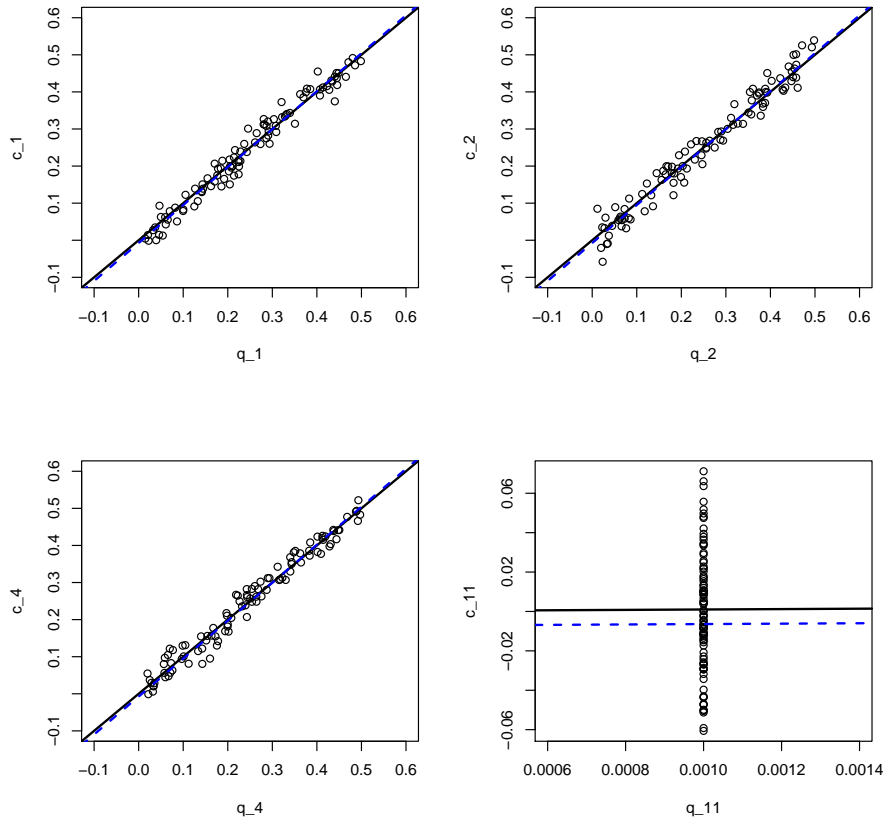


Figure 10: \mathbf{C} vs \mathbf{Q} , estimation for the LVR model. Known environmental effects topology.

PRESS PREDICTION

The PRESS perturbation experiment was modelled as an added value of 1 to the population growth rate of species 1,2,4, and 11, which was then multiplied by the environmental effect coefficient. In other words, the mean environmental covariate was increased by 1. The predicted difference in the ln-abundance abundance vector, in the MAR framework, is therefore computed as $(\mathbf{I} - \mathbf{B})^{-1} \mathbf{C} \Delta \mathbf{u}$.

As an example, here are typical values of the perturbation to the population growth rate (obtained for one randomly chosen parameter set):

$$\mathbf{C} \Delta \mathbf{u} = \begin{pmatrix} 0.489 \\ 0.268 \\ 0 \\ 0.083 \\ 0 \\ 0 \\ 0 \\ 0 \\ 0 \\ 0 \\ 0.006 \\ 0 \end{pmatrix}$$

This is therefore a relatively strong perturbation (but this order of magnitude is not unheard of). For basal elements affected by the environmental variable (species 1,2 and 4), the PRESS prediction performance for the Gompertz simulated food web model seems better than for the LVR model (compare Fig. 8, LVR, with Fig. 9,

Gompertz). Thus for basal species PRESS prediction is only hard with LVR dynamics. On the other hand, elements in the middle and top of the food web, that have weakly regulated dynamics, typically show outliers that impair the PRESS predictions in all cases: Gompertz and LVR, known and unknown food web and environmental effect topology⁵.

Clearly, as could be expected, the idea that MAR models can be used to predict the effects of PRESS perturbations may work only if those are extremely small (as a sort of sensitivity analysis, Gross & Edmunds, 2015), as any error in the identification of an effect tends to propagate through the \mathbf{B} matrix. It may be possible to consider only statistically significant elements in the \mathbf{B} and \mathbf{C} matrices, but as we have shown before, deciding which of these elements are non-zero based on the 95% CIs is somewhat prone to error. It would be better done using appropriate tools for perform model selection concurrently to estimation (e.g., the LASSO, Charbonnier *et al.*, 2010; Michailidis & d'Alché Buc, 2013; Basu *et al.*, 2015), which is a statistical endeavour unto itself and would require more evaluation (i.e., number of true positives, false positives, ROC curves, etc.).

⁵We do not show all the results because they are similar, PRESS predictions for LVR with unknown topology can be found here https://github.com/fbarraquand/MAR_foodWeb_MEE, version of record <https://zenodo.org/record/1218024>

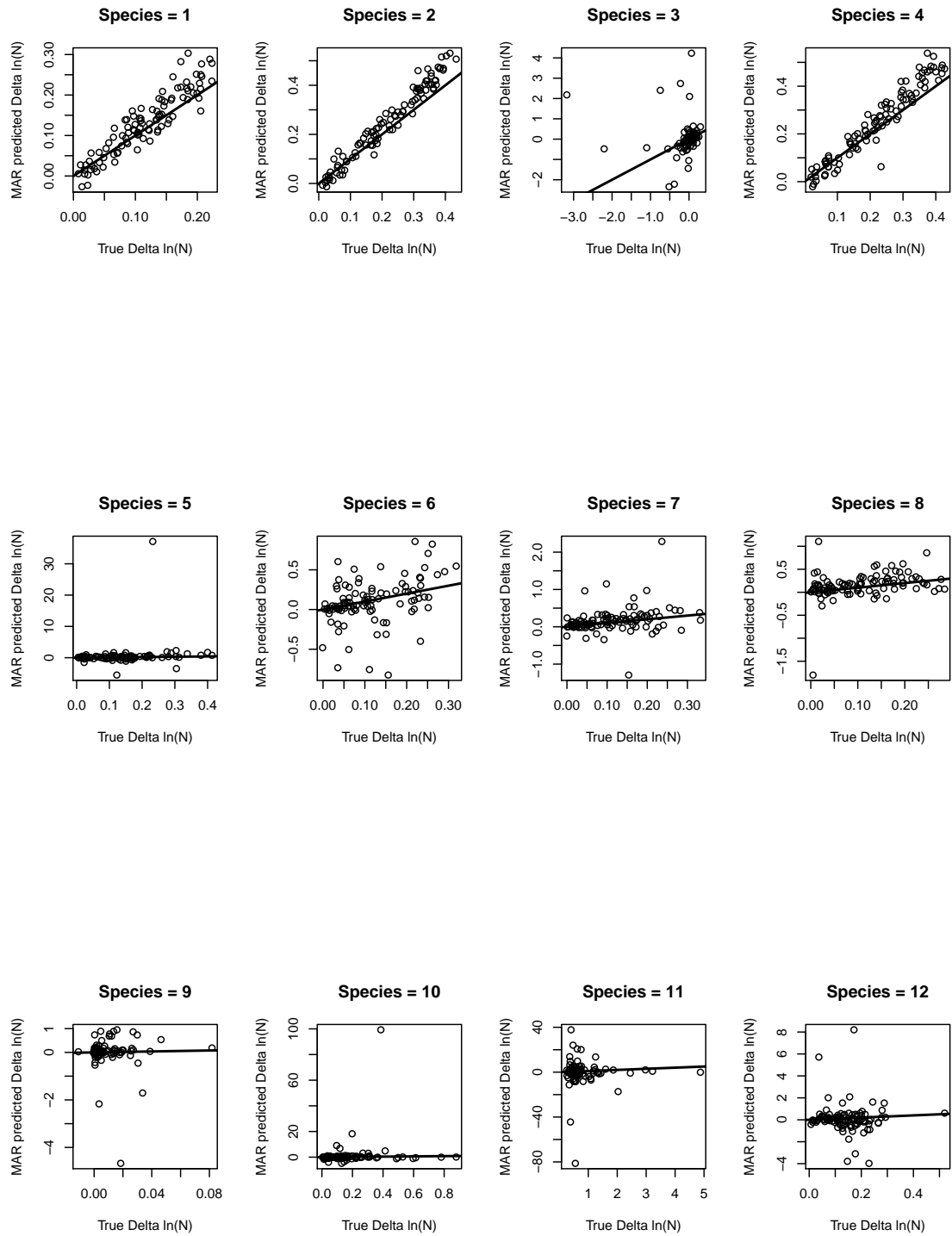


Figure 11: PRESS true values vs predictions, LVR model, known topology. Black line: $y = x$.

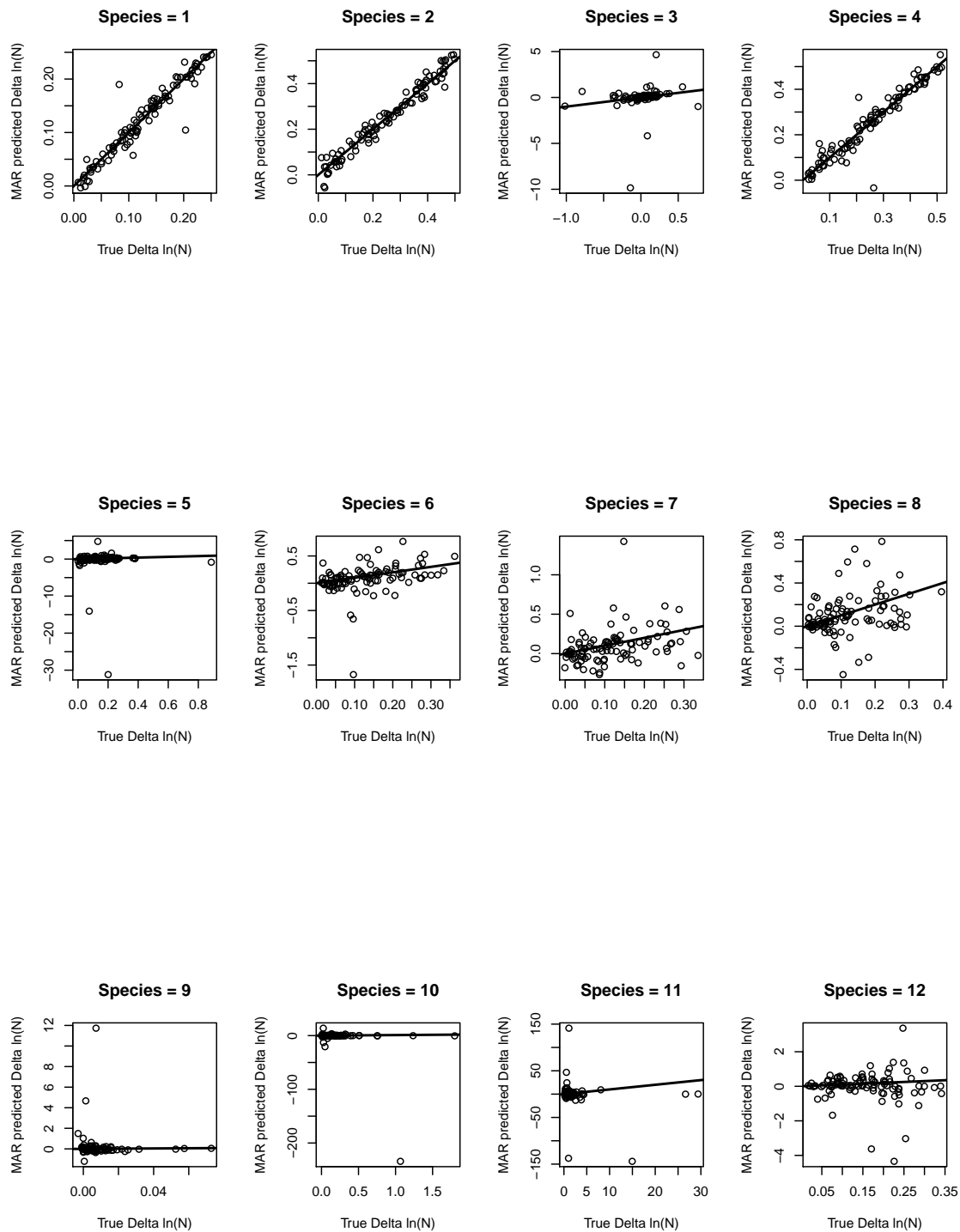


Figure 12: PRESS true values vs predictions, Gompertz model, known topology. Black line: $y = x$.

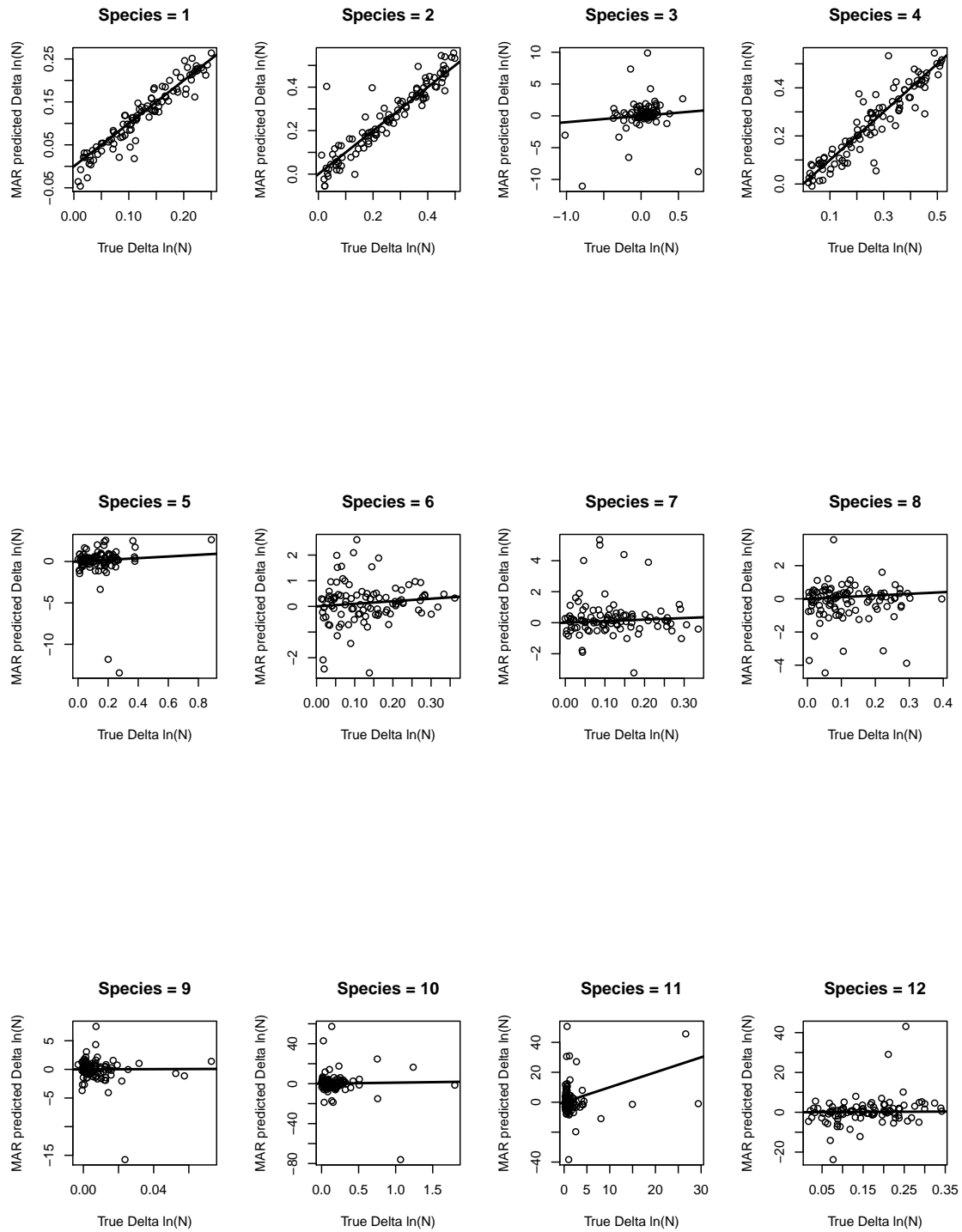


Figure 13: PRESS true values vs predictions, Gompertz model, unknown topology. Black line: $y = x$.

References

- Aufderheide, H., Rudolf, L., Gross, T. & Lafferty, K.D. (2013) How to predict community responses to perturbations in the face of imperfect knowledge and network complexity. *Proceedings of the Royal Society B: Biological Sciences*, **280**, 20132355.
- Basu, S., Michailidis, G. *et al.* (2015) Regularized estimation in sparse high-dimensional time series models. *The Annals of Statistics*, **43**, 1535–1567.
- Charbonnier, C., Chiquet, J. & Ambroise, C. (2010) Weighted-lasso for structured network inference from time course data. *Statistical applications in genetics and molecular biology*, **9**, 1–29.
- Erbach, A., Lutscher, F. & Seo, G. (2013) Bistability and limit cycles in generalist predator–prey dynamics. *Ecological Complexity*, **14**, 48–55.
- Gross, K. & Edmunds, P.J. (2015) Stability of Caribbean coral communities quantified by long-term monitoring and autoregression models. *Ecology*, **96**, 1812–1822.
- Holmes, E.E., Ward, E.J. & Scheuerell, M.D. (2014) Analysis of multivariate time-series using the MARSS package. Technical report.
- Michailidis, G. & d’Alché Buc, F. (2013) Autoregressive models for gene regulatory network inference: Sparsity, stability and causality issues. *Mathematical biosciences*, **246**, 326–334.
- Mutshinda, C.M., O’Hara, R.B. & Woiwod, I.P. (2011) A multispecies perspective on ecological impacts of climatic forcing. *Journal of Animal Ecology*, **80**, 101–107.
- Ovaskainen, O., Tikhonov, G., Dunson, D., Grøtan, V., Engen, S., Sæther, B. & Abrego, N. (2017) How are species interactions structured in species-rich communities? a new method for analysing time-series data. *Proceedings Biological sciences*, **284**.